Foxn1 maintains thymic epithelial cells to support T-cell development via *mcm2* in zebrafish

Dongyuan Ma[1], Lu Wang[1], Sifeng Wang[1], Ya Gao, Yonglong Wei, and Feng Liu[2]

State Key Laboratory of Biomembrane and Membrane Biotechnology, Institute of Zoology, Chinese Academy of Sciences, Beijing 100101, China

Edited by Max D. Cooper, Emory University, Atlanta, GA, and approved November 7, 2012 (received for review September 30, 2012)

The thymus is mainly comprised of thymic epithelial cells (TECs), which form the unique thymic epithelial microenvironment essential for intrathymic T-cell development. Foxn1, a member of the forkhead transcription factor family, is required for establishing a functional thymic rudiment. However, the molecular mechanisms underlying the function of Foxn1 are still largely unclear. Here, we show that Foxn1 functions in thymus development through Mcm2 in the zebrafish. We demonstrate that, in *foxn1* knockdown embryos, the thymic rudiment is reduced and T-cell development is impaired. Genome-wide expression profiling shows that a number of genes, including some known thymopoiesis genes, are dysregulated during the initiation of the thymus primordium and immigration of T-cell progenitors to the thymus. Functional and epistatic studies show that *mcm2* and *cdca7* are downstream of Foxn1, and *mcm2* is a direct target gene of Foxn1 in TECs. Finally, we find that the thymus defects in *foxn1* and *mcm2* morphants might be attributed to reduced cell proliferation rather than apoptosis. Our results reveal that the *foxn1-mcm2* axis plays a central role in the genetic regulatory network controlling thymus development in zebrafish.

The thymus is a central hematopoietic organ that produces mature T lymphocytes, one of the major players of the vertebrate adaptive immune system (1). In vertebrates, including zebrafish and mice, the thymus primordium is derived from the third pharyngeal endodermal pouch and then differentiates into functional cortical and medullary thymic epithelial cells (TECs) (1–4). TECs represent the primary functional cell type that forms the unique thymic epithelial microenvironment supporting T-cell differentiation. Therefore, the thymic epithelial microenvironment must be tightly controlled by extrinsic signals and intrinsic factors to support T-cell differentiation and maturation (5). Several signaling pathways and transcription factors have been demonstrated in thymus and T-cell development during vertebrate embryogenesis (4, 6–10).

Foxn1, Forkhead box protein N1, a winged-helix forkhead transcription factor, occupies a central position in the genetic network(s) that establishes a functional thymic rudiment (9, 11, 12). Foxn1$^{-/-}$ mice are athymic and hairless (9). Hypomorphic allele studies have suggested that Foxn1 is required for TEC development in both fetal and adult thymus in a dosage-dependent manner (13, 14). Conversely, overexpression of *foxn1* can improve the reduction in the populations of thymocytes and TECs in aged mice, therefore delaying age-associated thymic involution (15). The expression of zebrafish *foxn1* is initiated in the thymic primordium approximately 48 h after fertilization (hpf) and then gradually increases with the immigration of T-cell progenitors marked by *rag1* and *ikaros* (3, 4). Moreover, knockdown of the expression of *foxn1* in zebrafish embryos using antisense morpholinos impairs T-cell development (16).

Despite the essential function of *foxn1* in the early development of the thymus, there is limited understanding of its downstream targets and detailed regulatory mechanisms remain elusive. For example, previous studies have shown that *dll4* and chemokine ligand *ccl25* might be directly regulated by Foxn1 in mice and medaka (16). Chemokine signaling pathways (*ccl25*/*ccr9*, *cxcl12*/*cxcr4*) are thought to be important for attracting lymphoid progenitors (17), whereas the Notch pathway (*dll4*/*notch1*) is required for the specification of lymphoid progenitors toward the T-cell lineage (18, 19). However, other Foxn1-regulated downstream target genes have not yet been reported.

To investigate the function of *foxn1* during the development of thymus and T cells, we have used the zebrafish model to knock down *foxn1* expression by using antisense morpholinos (MO). Our data show that *foxn1*-deficient embryos display impaired expression of T-cell markers, whereas the expression of early TEC progenitor markers remains relatively unchanged. Expression profiling and functional analysis demonstrate that, besides the previously reported downstream target genes (such as *ccl25*) in medaka and mice, a unique *foxn1-mcm2* axis plays a pivotal role during the development of TECs and T cells in zebrafish.

Results

T-Cell Development Is Impaired in Zebrafish *foxn1* Morphants. Foxn1 has been demonstrated to be necessary in thymopoiesis in many vertebrates (9, 11, 16). To study the role of zebrafish Foxn1, antisense MOs (16) were used to knock down the expression of *foxn1* in zebrafish embryos. Then, whole mount in situ hybridization (WISH) and Western blotting were carried out to check the endogenous expression of zebrafish *foxn1* mRNA and the encoded protein Foxn1. We found that both the levels of *foxn1* mRNA and Foxn1 protein were down-regulated in the zebrafish embryos injected with 4 ng of *foxn1* MOs (Fig. 1 *A* and *B*). When *foxn1* MOs were injected into a *rag2:*dsRed transgenic line at the one cell stage, the numbers of the dsRed^{+} T cells were significantly decreased at 5 dpf (Fig. 1*C*). Compared with the control, the expression of several T-cell markers including *rag1*, *il7r*, and *ikaros* was remarkably decreased in the thymus of zebrafish *foxn1* morphants at 4 dpf (Fig. 1*D*). Quantitative RT-PCR (qPCR) further confirmed the WISH data (Fig. 1*E*). Moreover, when *foxn1* was knocked down in a *cmyb*:GFP transgenic line, the population of the GFP^{+} T cells in the thymus was greatly reduced, whereas the numbers of the GFP^{+} hematopoietic progenitors in the pronephros (the equivalent of bone marrow in mammals) and caudal hematopoietic tissue (the equivalent of fetal liver in mammals) at 4 dpf were not changed in *foxn1* morphants (Fig. S1*A*) (20). In addition, a parathyroid marker, *gcm2*, was unchanged in *foxn1* morphants (Fig. S1*B*). These results suggest a role for *foxn1* in thymus, which is consistent with data in mice. Moreover, *epcam*, and *hoxa3a*, appeared unchanged in *foxn1* morphants (Fig. S2*A*). These data are consistent with the observation that these genes act earlier than *foxn1* during thymus development in mouse (5, 10). Previous work showed that thymus homing was defective in zebrafish *foxn1* morphants because of the down-regulation of chemokine/chemokine receptors (16). Here, expression of chemokine and

Author contributions: D.M. and F.L. designed research; D.M., L.W., S.W., Y.G., and Y.W. performed research; D.M., L.W., and F.L. analyzed data; and F.L. wrote the paper.

The authors declare no conflict of interest.

This article is a PNAS Direct Submission.

[1]D.M., L.W., and S.W. contributed equally to this work.

[2]To whom correspondence should be addressed. E-mail: liuf@ioz.ac.cn.

This article contains supporting information online at www.pnas.org/lookup/suppl/doi:10.1073/pnas.1217021110/-/DCSupplemental.

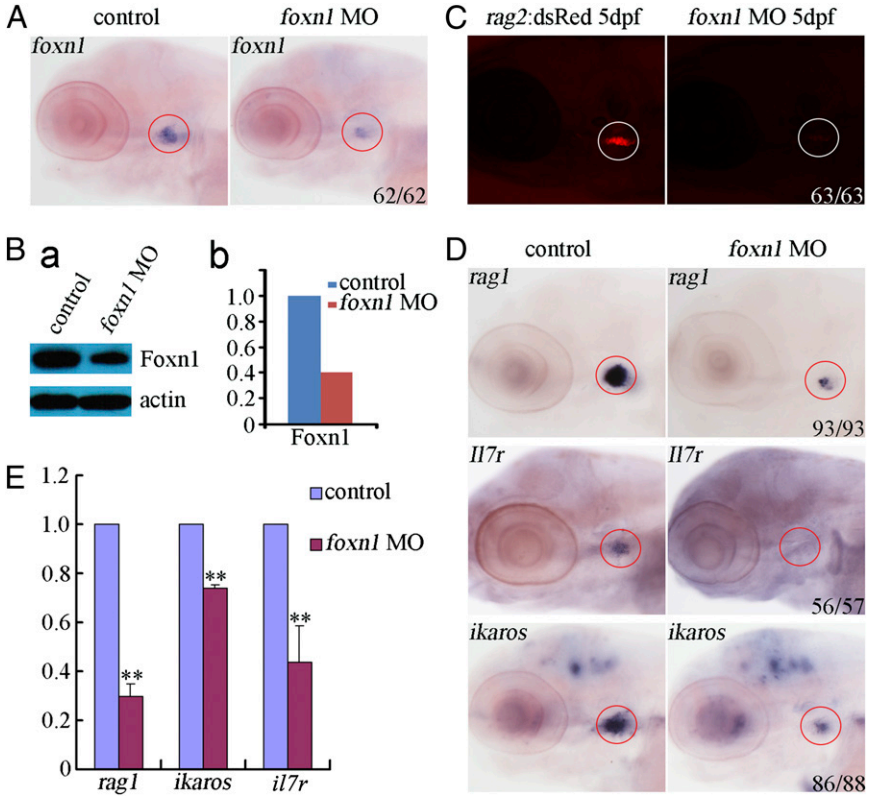

Fig. 1. T-cell development is impaired in zebrafish *foxn1* morphants. (*A* and *B*) The endogenous expression level of *foxn1* transcript and the encoded protein in zebrafish *foxn1* morphants at 4 dpf detected by WISH (*A*) and Western blot (*B*). *Ba*, Western blot; *Bb*, Western blot results were quantified by using Quantity 1 software. (*C*) The *rag2*:dsRed expression was abolished in *foxn1* morphants at 5 dpf. (*D*) The expression of lymphocyte markers, including *rag1*, *il7r*, and *ikaros*, was down-regulated in the thymus in zebrafish *foxn1* morphants. Anterior to the left and dorsal to the top; circles mark the thymus. (*E*) qRT-PCR results showing that the expression of *rag1*, *il7r*, and *ikaros* is down-regulated in zebrafish *foxn1* morphants (mean ± SD, *t* test, $^{**}P < 0.01$, $n = 3$).

chemokine receptor was also examined. We found that the expression of *ccr9b* and *ccl25a* was both decreased in *foxn1* morphants at 4 dpf (Fig. S2*B*). Taken together, knockdown of *foxn1* expression impairs T-cell development in zebrafish embryos.

Expression of *mcm2*, *cdca7*, *cbfb*, and *runx3* Is Specifically Down-Regulated in the Thymus of Zebrafish *foxn1* Morphants. Although *foxn1* is pivotal in establishing a functional thymic rudiment, there is limited understanding of its downstream targets. To further study the molecular mechanism of *foxn1* in thymopoiesis, microarray experiments were carried out. Zebrafish thymus collected at two stages, 2 dpf and 4 dpf, were analyzed because the thymic anlage forms from the pharyngeal endoderm at 2 dpf and lymphopoiesis initiates after the expression of *rag1* at 4 dpf. According to the microarray data, 310 genes were up-regulated, whereas 466 genes were down-regulated at 2 dpf, and 379 genes were up-regulated, whereas 369 genes were down-regulated at 4 dpf (Fig. S3 *A* and *B*). The expression of a list of selected genes was further verified by RT-PCR and transverse sections after WISH (Fig. S3 *C* and *D*). Among them, the expression of *cbfb*, *cdca7*, *mcm2*, and *runx3* was specifically decreased in the thymus in zebrafish *foxn1* morphants (Fig. 2*B*, circles mark the thymus area). qPCR confirmed the decrease of these genes in thymus tissue at 4 dpf (Fig. 2*A*). Furthermore, immunoblotting analysis indicated that the protein levels of Cbfb, Cdca7, Mcm2, and Runx3 were all decreased (Fig. 2*C*).

Minichromosome maintenance complex component 2 (Mcm2) is a key component of the prereplication complex and involved in the initiation of eukaryotic genome replication (21, 22). Cell division cycle associated 7 (Cdca7) is a c-Myc target gene, which is expressed in adult thymus and small intestine (23, 24). Runx3 and Cbfb have been reported to be expressed in mouse T lymphocytes (25, 26). The detailed expression pattern of these four genes in zebrafish was examined by using WISH in *cloche* mutant, which contains no blood including lymphoid cells, although a few TECs still exist according to the expression of *foxn1* (Fig. S4*A*). Our results show that the absence of *runx3* and reduced *cbfb* expression was detected in the thymus, whereas *cdca7* and *mcm2* were still expressed in the thymus of the *cloche* mutant at 4 dpf (Fig. S4*A*). Transverse sections of WISH embryos at 4 dpf clearly demonstrated their expression in the thymus was reduced in *foxn1* morphants compared with controls (Fig. S4*B*). To determine whether these genes were also expressed in TECs and/or T cells in mammals, we examined their expression in mouse thymus tissue and TEC lines. By RT-PCR, expression of *cdca7* and *mcm2* but not *runx3* was detected in two mouse TEC lines, 4c18 and 1c6, whereas all four genes were expressed in mouse thymus tissue (Fig. S4*C*). Together, these results show that the four candidate genes were specifically decreased in the thymus of zebrafish *foxn1* morphants and *cdca7* and *mcm2* were expressed in TECs in both zebrafish and mice.

T-Cell Development Is Impaired in Zebrafish *mcm2* and *cdca7* Morphants. To study the role of Mcm2 and Cdca7 in thymopoiesis and T-cell development, translation blocking MOs were designed to knock down the expression of these genes in zebrafish embryos. Western blotting analysis indicated that compared with the control, the levels of Cdca7 and Mcm2 were decreased in their respective morphants injected with 4 ng of individual MOs (Fig. 3*A*). qPCR and WISH showed that in *mcm2* morphants at 4 dpf, the expression of lymphoid progenitors and T-cell markers, including *rag1*, *ikaros*, and *il7r* was greatly reduced in the thymus

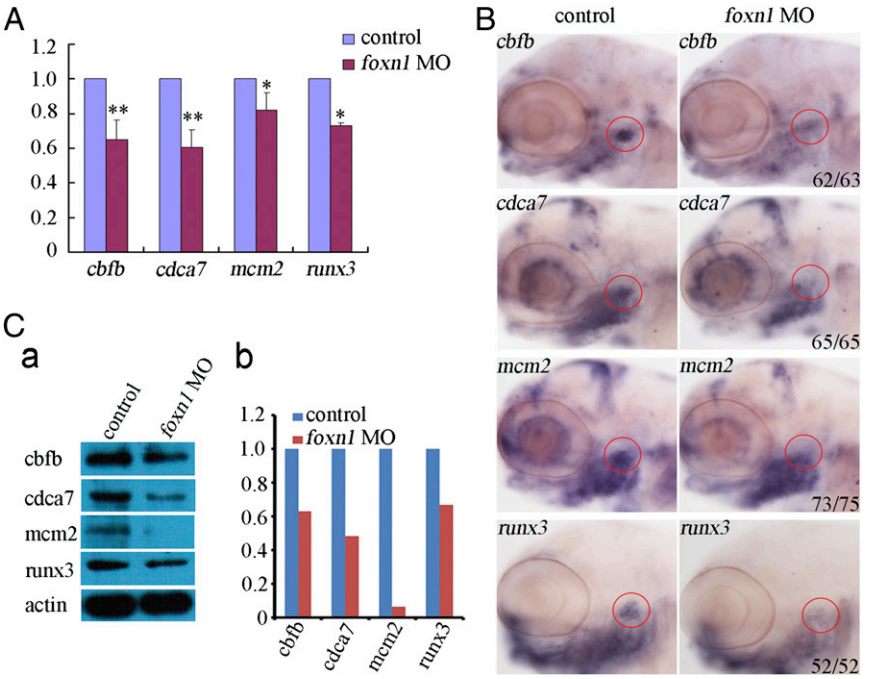

Fig. 2. Four genes are specifically decreased in the thymus in zebrafish *foxn1* morphants. (*A*–*C*) The expression level of *cbfß*, *cdca7*, *mcm2*, and *runx3* in the thymus in zebrafish *foxn1* morphants using qRT-PCR (*A*; mean ± SD, Student's *t* test, $*P < 0.05$, $**P < 0.01$, $n = 3$), WISH (*B*), and Western blot (*C*), respectively. *Ca*, Western blot; *Cb*, Western blot results were quantified by using Quantity one software. Anterior to the left and dorsal to the top; circles mark the thymus.

(Fig. 3 *B* and *C*). However, the expression of TEC marker *foxn1* was condensed at 4 dpf and was dramatically reduced in *mcm2* morphants at 5 dpf (Fig. 3*C* and Fig. S5*B*). Similarly, in *cdca7* morphants at 4 dpf, expression of *rag1*, *ikaros*, and *il7r* was dramatically decreased in the thymus (Fig. 3 *B* and *C*), whereas the expression patterns of *foxn1* were slightly decreased at 4 dpf and greatly reduced at 5 dpf (Fig. 3*C* and Fig. S5*B*). Interestingly, both the thymus expression of *cbfb* and *runx3* was absent or severely attenuated in *mcm2*- or *cdca7* morphants (Fig. S5*A*), consistent with the impaired T-cell development in these two morphants, and *runx3* and *cbfb* could be used as T-cell markers in zebrafish. To confirm the specificity of *mcm2* and *cdca7* atg MOs, we designed second-splice MO for *mcm2* and *cdca7*. RT-PCR showed that endogenous wild-type transcript was reduced in *mcm2* splice MO injected embryos, whereas there was a new band in the *cdca7* splice MO injected embryos due to intron retention (Fig. S5*C*). WISH showed that the expression of *rag1* and *ikaros* was reduced in both *mcm2* and *cdca7* splice MO injected embryos similar to atg MO injected embryos (Fig. S5 *C* and *D* and Fig. 3*C*), suggesting the T-cell defects were specific to the deficiency of *mcm2* or *cdca7*. Taken together, T-cell development is impaired in zebrafish *mcm2* and *cdca7* morphants.

Mcm2/Cdca7 Function Downstream of Foxn1 Controlling T-Cell Development. To determine whether *mcm2* and *cdca7* act downstream of *foxn1* in controlling thymopoiesis and T-cell development, we performed rescue experiments by overexpression of individual or combined genes in *foxn1* morphants. The expression of *rag1* and *ikaros* was modestly rescued in *foxn1* morphants by overexpression of single individual genes (Fig. 4 *A* and *B*). However, overexpression of both *mcm2* and *cdca7* mRNAs rescued the expression of *ikaros* and *rag1* expression in *foxn1* morphants at 4 dpf (Fig. 4 *A* and *B*), suggesting that Mcm2 and Cdca7 may work together in TECs. To demonstrate that the specific rescue of the T-cell lineage was not due to the increased Foxn1 expression, we examined endogenous Foxn1 protein levels in embryos injected with *mcm2* and *cdca7* mRNA, individually or combinatorially (Fig. 4*C*). As shown by Western blotting, expression of Foxn1 was consistently decreased in the *foxn1* morphants without or with ectopic expression of *mcm2* and/or *cdca7* (Fig. 4*C*), confirming that the specific rescue was due to the injected mRNAs. The incomplete rescue of *ikaros* expression in *foxn1* morphants (Fig. 4*B*) suggests that, besides *mcm2* and *cdca7*, there might be other unidentified *foxn1* targets involved in Foxn1-dependent thymus development (Fig. 4 *A* and *B*).

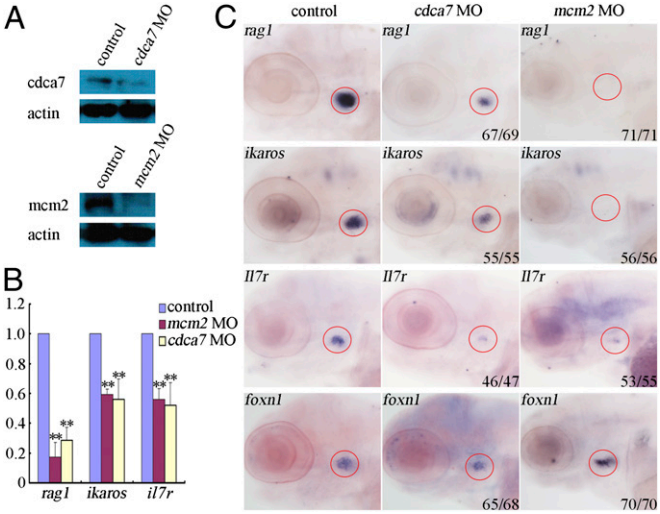

Fig. 3. T-cell development is impaired in zebrafish *cdca7* and *mcm2* morphants. (*A*) The protein expression of Cdca7 and Mcm2 in the zebrafish *cdca7* and *mcm2* morphants detected by using Western blot. (*B*) The expression of T-cell markers (*rag1*, *il7r*, and *ikaros*) in zebrafish *cdca7* and *mcm2* morphants by qRT-PCR (mean ± SD, Student's *t* test, $**P < 0.01$, $n = 3$). (*C*) The expression of *rag1*, *il7r*, *ikaros*, and *foxn1* in zebrafish *cdca7* and *mcm2* morphants by WISH. Anterior to the left and dorsal to the up; circles mark the thymus.

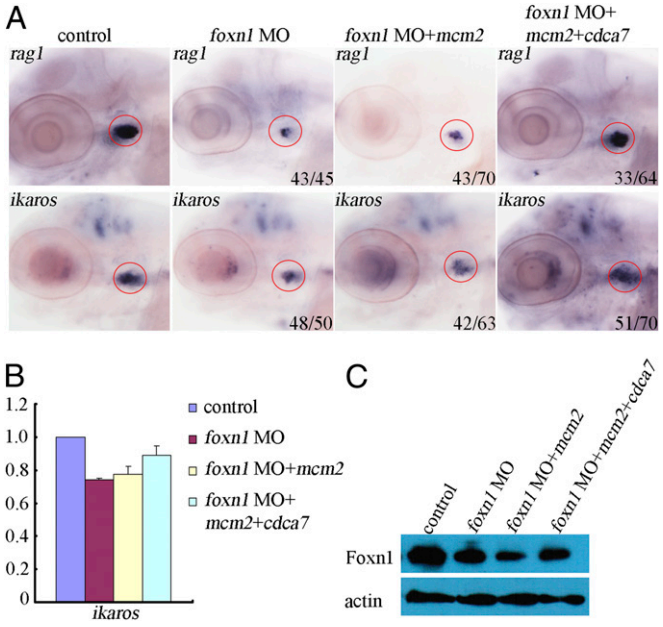

Fig. 4. The expression of *rag1* and *ikaros* can be rescued in *foxn1* morphants coinjected with mRNAs. (*A*) The expression of *rag1* and *ikaros* in *foxn1* morphants coinjected with mRNAs using WISH. (*B*) The expression of *ikaros* in *foxn1* morphants coinjected with mRNAs using qRT-PCR (mean ± SD, $n = 3$). (*C*) The protein level of Foxn1 in *foxn1* morphants coinjected with mRNAs.

***mcm2* Is a Direct Downstream Target of Foxn1.** To examine whether *mcm2* was a direct downstream target of Foxn1, we performed chromosome immunoprecipatation (ChIP) assays. It was shown that the fragments of the *mcm2* promoter containing consensus Foxn1 binding sites were significantly enriched in Foxn1 binding (Fig. 5*A*). Furthermore, the ChIP assay was performed in *foxn1* morphants to demonstrate that the specific enrichment of Foxn1 binding on the *mcm2* promoter was truly Foxn1 dependent. It is clear that Foxn1 was significantly enriched in control but not in *foxn1* morphants by qRT-PCR (Fig. 5*B*). Therefore, Foxn1 can directly bind to the promoter region of *mcm2* in vivo.

To further demonstrate that the consensus Foxn1 binding sites can functionally respond to *foxn1* expression, we generated *mcm2* promoter constructs with or without the conserved Fox binding sites (Fig. 5*C*) and transfected them into the human embryonic kidney cell line HEK293. As shown in Fig. 5*C*, luciferase activity was increased in a dose-dependent manner when cotransfected with pCDNA3.1(+)-*foxn1* and *mcm2* promoter but not with a truncated *mcm2* promoter (*mcm2p*), suggesting that Foxn1 can promote *mcm2* expression through the conserved binding sites in the promoter region. Taken together, these data demonstrate that *mcm2* is a direct target of *foxn1*.

Impaired T-Cell Development in *mcm2* Morphants Is Due to Decreased Cell Proliferation Rather than Apoptosis. The impaired T-cell development in zebrafish *foxn1* or *mcm2* morphants might be attributed to abnormal apoptosis. To explore this possibility, we used the TUNEL assay. We found that apoptosis in *mcm2* morphants was increased ectopically, whereas only a slight increase was found in *foxn1* morphants (Fig. S6*A*). Therefore, the increased apoptosis in the *mcm2* morphants might be one of reasons why T-cell development was affected. P53 deficiency as a result of *p53* MO knockdown or genetic mutation of the *p53* gene can efficiently inhibit excessive apoptosis in zebrafish morphants or mutants (27, 28). Therefore, *p53* MO was coinjected with *mcm2* MO to prevent *p53*-dependent apoptosis. The ectopic TUNEL signals in the *mcm2* morphants were reduced back to the normal level of control embryos by coinjection of *p53* MO, suggesting that apoptosis was inhibited effectively (Fig. S6*A*). However, the expression of *rag1* and *ikaros* was not rescued in those embryos (Fig. S6 *B* and *C*). Thus, the impaired T-cell development in *mcm2* morphants was not due to excessive apoptosis of TECs or early T-cell progenitors.

The down-regulation of *mcm2* and *cdca7* in *foxn1* morphants suggests that cell proliferation might be affected. In mice, Foxn1 is known to regulate proliferation of TECs (13). Therefore, we first examined cell proliferation in *foxn1* or *mcm2* morphants by anti-BrdU labeling. The results clearly showed that anti-BrdU signals remarkably reduced in the thymus region in both *foxn1*

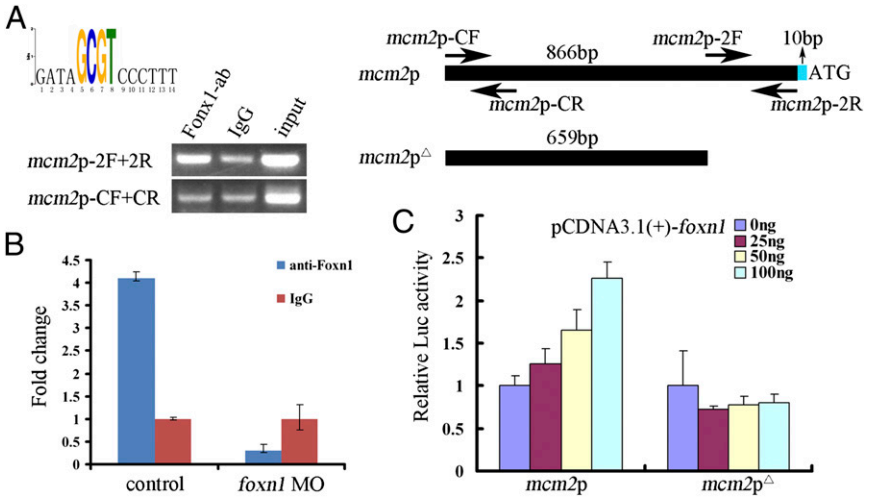

Fig. 5. *mcm2* is a direct target of Foxn1. (*A*) Predicted Foxn1 binding site and ChIP-PCR analysis of the Foxn1 binding to the promoter region of *mcm2*. The consensus site was marked by colored letters. (*B*) qRT-PCR analysis of Foxn1 binding to the promoter region of *mcm2* in control and *foxn1* morphants (mean ± SD, $n = 3$). (*C*) The *mcm2* promoter and the *mcm2p* truncated constructs, and the luciferase reporter assay (mean± SD, $n = 3$). HEK293 cells were cotransfected by the Renilla reporter plasmid and the *mcm2* promoter construct together with pCDNA3.3(+)-*foxn1*. Luciferase assays were determined by using the Dual-Luciferase Reporter Assay System (Promega). 2F/2R stand for a pair of gene specific primers spanning the Foxn1 binding site; CF/CR stand for control primers. The results indicate that the functional consensus Fox binding sites of the *mcm2* promoter are positively regulated by Foxn1 in a dose-dependent manner.

and *mcm2* morphants, and these results were confirmed by quantification (Fig. 6 *A* and *B*). To further verify these data, we used anti–Pan-CK, a well-known marker for TECs in mouse, to visualize TECs in the zebrafish thymus. As shown in Fig. 6*C*, both the thymus size and the TEC number were severely reduced in *foxn1* and *mcm2* morphants compared with controls. To get better resolution of the thymus structure, we turned to transmission electron microscopy. As shown in Fig. S7, both TECs and T lymphocytes in the thymus of *foxn1* and *mcm2* morphants were compromised. The morphology of TECs in the *foxn1* and *mcm2* morphants was blunter compared with the reticular shape in control embryos. This result is consistent with the recent finding reported by Hess and Boehm (29), suggesting that the interaction between TECs and T cells regulates TEC shape. Cell counting on the sections with 5–10 embryos per sample confirmed the marked decrease of cell number for both cell types (Fig. S7*C*). Taken together, these results suggested that the thymus defects in both morphants were most likely attributed to a decrease in cell proliferation rather than altered apoptosis (Fig. 6*D*).

Discussion

Our data indicate that *foxn1* knockdown in zebrafish results in impaired T-cell development. Microarray analysis showed that a number of genes were dysregulated and, among those, some are well-defined thymus-related genes including chemokine genes and many known T-cell-specific genes. Importantly, functional analysis and genetic rescue experiments demonstrated that a *foxn1-mcm2* axis is responsible for the T-cell defects in the *foxn1* morphants. We also showed that the T-cell defects in the *foxn1* knockdown embryos were more likely attributed to reduced cell proliferation, rather than altered apoptosis, which disrupts the thymic epithelial niche for proper T-cell development.

The interaction between TECs and developing thymocytes is critical for proper development of a functional thymus and maturation of T cells (1). The phenotype of knockdown of *foxn1* in zebrafish we reported here is consistent with previous findings that *foxn1* regulates TEC development in a dose-dependent manner in both fetal and adult thymus (13, 14). Alternatively, there might be other transcriptional regulators controlling TEC differentiation, besides Foxn1 itself (5). The condensation of *foxn*1 and other TEC markers in the thymus of *foxn1* morphants agrees with previous reports using *foxn1* hypomorphic mice, which mimic the "involution" of the thymus in normal aging mice (30, 31). In contrast, overexpression of Foxn1 can delay age-related thymic involution (15). However, whether the shrinking of the thymus in the *foxn1* morphants is the cause or the consequence of T-cell impairment is still debatable. It seems reasonable that *foxn1* deficiency prevents thymocyte homing (as shown by down-regulation of *ccl25*) and differentiation (down-regulation of *ikaros*, *rag1*), and causes maintenance defects in the TEC microenvironment (via *mcm2* and *cdca7* to regulate cell proliferation) (Fig. 6*D*). Subsequently, the lack of thymocytes in the thymus would break down the compartmentation of the thymus structure. Therefore, the interdependence between TECs and T cells, together with their cell-autonomous effects that are exerted by cell intrinsic signaling and molecules, make a tightly controlled system of thymic epithelial niches and the thymocytes.

The forkhead transcription factor, Foxn1, is a well-known master regulator of thymus development and is expressed in all TECs during thymus organogenesis (1, 9, 11). To fulfill the proper interaction between TECs and T cells, the regulation of *foxn1* must incorporate signaling (such as BMP and WNT), from neighboring mesenchyme or other stromal cells plus transduction of the instructive signal flow to the thymocytes (4, 7). How the information flow from TECs to T cells is regulated is of great interest and is still being elucidated. A previous report suggests that in vertebrates, Foxn1 can regulate *dll4*/*notch* and chemokine ligand *ccl25*/*ccr9* signaling to influence the outcome of T-cell development (16). Our data here show that Foxn1, as a key regulator of TECs, can regulate an array of downstream targets to ensure proper development of T cells within the thymic epithelial niche. Specifically, we found that Foxn1 can directly regulate a component of the DNA replication-related complex, Mcm2, and Cdca7 specifically in TECs, implying maintenance and/or expansion of TECs might be affected. Our work demonstrated that *mcm2* is directly regulated by *foxn1*, and overexpression of *mcm2* and *cdca7* can rescue the *foxn1* knockdown defects, suggesting that these two genes are bona fide downstream targets of *foxn1* in thymopoiesis. The replication–licensing complex containing Mcm2 is essential for DNA replication during cell cycle and the *foxn1*-deficiency–caused *mcm2* defect would certainly compromise TEC proliferation, therefore disrupting the thymic epithelial environments to support T-cell development. In addition, the incomplete rescue by *mcm2* and *cdca7* overexpression indicates that other *foxn1* targets might also be involved in *foxn1*-dependent thymopoiesis. Therefore, the detailed molecular mechanism underlying *foxn1* function in thymopoiesis, especially the interaction between TECs and T-cell development in vertebrates, need further exploration.

In summary, we have characterized the detailed phenotypes of *foxn1*-deficient zebrafish embryos and discovered an expanded list of *foxn1* downstream genes. Our studies emphasized that *foxn1* regulates TEC–T-cell interaction through a unique *foxn1-mcm2* axis. The finding reported here will further improve our understanding of the molecular mechanism of *foxn1* function,

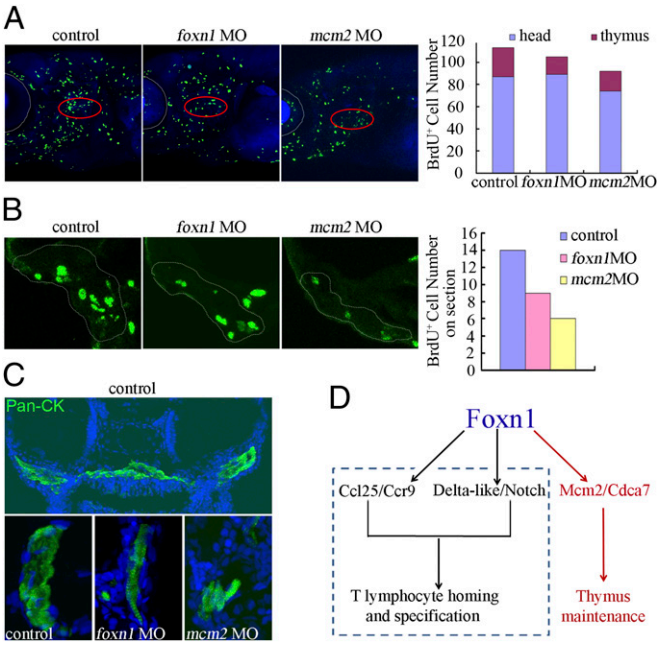

Fig. 6. TEC proliferation defects in *foxn1* and *mcm2* morphants by BrdU labeling. (*A*) Reduced anti–BrdU-positive cells in *foxn1*- and *mcm2* morphants by BrdU labeling on whole mount. Anti-BrdU positive cells were quantified in the thymus and the head region without the thymus of controls ($n = 15$), *foxn1* morphants ($n = 23$), and *mcm2* morphants ($n = 19$). Green, anti–BrdU-positive cells; blue, DAPI staining. Circles indicate thymus. (*B*) Reduced anti–BrdU-positive cells in control, *foxn1* morphants, and *mcm2* morphants by BrdU labeling on thymus sections. Dotted lines indicate the thymus area. Section thickness, 10 μm. The average number of anti–BrdU-positive cells per section was quantified. (*C*) Immunofluorescence on thymus sections with anti–Pan-CK staining, which clearly showed reduced number of TECs and smaller size of thymus in *foxn1* and *mcm2* morphants, compared with controls. Green, Pan-CK staining; blue, DAPI staining. (*D*) A proposed model of foxn1 functions in thymus development. Dashed square, published data; red arrows, this work.

which might provide useful insights for medical intervention of early degeneration of thymus and T lymphocytes (32).

Materials and Methods

Fish Strains and Embryos. Zebrafish embryos were obtained by natural spawning of adult Tubingen strain zebrafish. Embryos were raised and maintained at 28.5 °C in system water. *rag2:*dsRed and *cmyb:*GFP transgenic lines were kindly provided by Zilong Wen (Hong Kong University of Science and Technology, Hong Kong, China) and Anming Meng (Tsinghua University, Beijing, China), respectively. This study was approved by the Ethical Review Committee in the Institute of Zoology, Chinese Academy of Sciences.

Morpholinos, Primers, mRNA Synthesis, Microinjection, and WISH. Standard MOs and antisense MOs were purchased from GeneTools and prepared as 1 mM stock solutions by using ddH_2O. All of the gene-specific MOs and the primers used for full coding sequence (CDS) amplification and promoter cloning were described in Table S1. Capped fish full-length mRNAs for injection were synthesized in vitro by using the mMessage mMachine SP6 kit according to the instruction manual (Ambion). MOs (4 ng for atg MOs and 5 ng for splice MOs) and capped mRNA (100 pg) were injected alone or in combination into one or two cell stage zebrafish embryos at the yolk/blastomere boundary. WISH for zebrafish embryos was performed as described (33).

Western Blot Analysis. The thymus of zebrafish embryos at 4 dpf were dissected as above and homogenized with a 1-mL syringe and needle in lysis buffer (10 mM Tris·HCl at pH 8.0, 10 mM NaCl, and 0.5% Nonidet P-40) containing protease inhibitor (Roche). Western blot was carried out as described (34). Rabbit polyclone zebrafish Foxn1 antibody was made by AbMax Biotechnology. Antibodies for actin (Cell Signaling; 4967), Cbfß (ab33516), Cdca7 (ab69609), Mcm2 (BD Pharmingen; 559541), Runx3 (ab68938), pHistone H3 (Cell Signaling; 9701), anti-mouse secondary antibody (115-035-003), and anti-rabbit secondary antibody (111-035-003) were bought from Abcam, Cell Signaling, BD Pharmingen, and Jackson ImmunoResearch Laboratories, respectively.

ChIP Assay and qPCR. ChIP analysis was carried out with the thymus region of wild-type embryos or *foxn1* morphants at 4 dpf as described (34). Rabbit polyclonal zebrafish Foxn1 antibody made by AbMax Biotechnology was used for immunoprecipitation with IgG as negative control. The primers specific and unspecific to the Foxn1 binding site in the upstream regions of genes were summarized in Table S1. The CF and CR represent for control forward and control reverse primers, respectively. All of the PCR products were approximately 200 bp and were evaluated on a 2% (wt/vol) agarose gel. qPCR was carried out by using the GoTaq qPCR Master Mix (Promega) on the Bio-Rad CFX96 Real-Time PCR system. All of the primers used for qRT-PCR were described in Table S2. All of the experiments were repeated three times in triplicate and the results were analyzed as described (34). Data were represented as mean ± SD and Student's *t* test was performed for comparison between control and experimental groups.

TUNEL, BrdU Labeling, Microarray, and Transmission Electron Microscopy Assay. TUNEL assay were performed as described (34). For details about BrdU labeling, microarray, and transmission electron microscopy (TEM), see *SI Materials and Methods*.

Statistical Analysis. For statistical analysis, Student's unpaired two-tailed *t* test was used for all comparisons.

ACKNOWLEDGMENTS. We thank Drs. Nancy Manley, Roger Patient, and Qing Ge for advice and critical reading of the manuscript; Drs. Nikolaus Trede and Sarah Hutchinson for sharing BrdU labeling protocol; Dr. Yong Zhao for providing anti–Pan-CK antibody, mouse thymus tissue, and TEC lines; the core facilities bioimaging laboratory at the Institute of Biophysics [Chinese Academy of Sciences (CAS)], for electron microscopy work; and Sufeng Sun for his help with analyzing TEM images. This work was supported by National Basic Research Programs of China Grants 2010CB945300 and 2011CB943900, National Science Foundation of China Grants 30971678 and 31000647, and Strategic Priority Research Program of the CAS Grant XDA01010110.

1. Rodewald H-R (2008) Thymus organogenesis. *Annu Rev Immunol* 26(1):355–388.
2. Manley NR (2000) Thymus organogenesis and molecular mechanisms of thymic epithelial cell differentiation. *Semin Immunol* 12(5):421–428.
3. Willett CE, Cortes A, Zuasti A, Zapata AG (1999) Early hematopoiesis and developing lymphoid organs in the zebrafish. *Dev Dyn* 214(4):323–336.
4. Soza-Ried C, Bleul CC, Schorpp M, Boehm T (2008) Maintenance of thymic epithelial phenotype requires extrinsic signals in mouse and zebrafish. *J Immunol* 181(8): 5272–5277.
5. Ma D, Wei Y, Liu F (December 29, 2011) Regulatory mechanisms of thymus and T cell development. *Dev Comp Immunol*, 10.1016/j.dci.2011.12.013.
6. Tsai PT, Lee RA, Wu H (2003) BMP4 acts upstream of FGF in modulating thymic stroma and regulating thymopoiesis. *Blood* 102(12):3947–3953.
7. Balciunaite G, et al. (2002) Wnt glycoproteins regulate the expression of FoxN1, the gene defective in nude mice. *Nat Immunol* 3(11):1102–1108.
8. Manley NR, Condie BG (2010) Transcriptional regulation of thymus organogenesis and thymic epithelial cell differentiation. *Prog Mol Biol Transl Sci* 92:103–120.
9. Nehls M, Pfeifer D, Schorpp M, Hedrich H, Boehm T (1994) New member of the winged-helix protein family disrupted in mouse and rat nude mutations. *Nature* 372(6501):103–107.
10. Gordon J, Manley NR (2011) Mechanisms of thymus organogenesis and morphogenesis. *Development* 138(18):3865–3878.
11. Corbeaux T, et al. (2010) Thymopoiesis in mice depends on a Foxn1-positive thymic epithelial cell lineage. *Proc Natl Acad Sci USA* 107(38):16613–16618.
12. Schorpp M, et al. (2002) A zebrafish orthologue (whnb) of the mouse nude gene is expressed in the epithelial compartment of the embryonic thymic rudiment. *Mech Dev* 118(1-2):179–185.
13. Chen L, Xiao S, Manley NR (2009) Foxn1 is required to maintain the postnatal thymic microenvironment in a dosage-sensitive manner. *Blood* 113(3):567–574.
14. Nowell CS, et al. (2011) Foxn1 regulates lineage progression in cortical and medullary thymic epithelial cells but is dispensable for medullary sublineage divergence. *PLoS Genet* 7(11):e1002348.
15. Zook EC, et al. (2011) Overexpression of Foxn1 attenuates age-associated thymic involution and prevents the expansion of peripheral CD4 memory T cells. *Blood* 118(22): 5723–5731.
16. Bajoghli B, et al. (2009) Evolution of genetic networks underlying the emergence of thymopoiesis in vertebrates. *Cell* 138(1):186–197.
17. Bleul CC, Boehm T (2000) Chemokines define distinct microenvironments in the developing thymus. *Eur J Immunol* 30(12):3371–3379.
18. Hozumi K, et al. (2008) Delta-like 4 is indispensable in thymic environment specific for T cell development. *J Exp Med* 205(11):2507–2513.
19. Koch U, et al. (2008) Delta-like 4 is the essential, nonredundant ligand for Notch1 during thymic T cell lineage commitment. *J Exp Med* 205(11):2515–2523.
20. Bertrand JY, et al. (2010) Haematopoietic stem cells derive directly from aortic endothelium during development. *Nature* 464(7285):108–111.
21. Chen S, Bell SP (2011) CDK prevents Mcm2-7 helicase loading by inhibiting Cdt1 interaction with Orc6. *Genes Dev* 25(4):363–372.
22. Nishiyama A, Frappier L, Méchali M (2011) MCM-BP regulates unloading of the MCM2-7 helicase in late S phase. *Genes Dev* 25(2):165–175.
23. Prescott JE, et al. (2001) A novel c-Myc-responsive gene, JPO1, participates in neoplastic transformation. *J Biol Chem* 276(51):48276–48284.
24. Osthus RC, et al. (2005) The Myc target gene JPO1/CDCA7 is frequently overexpressed in human tumors and has limited transforming activity in vivo. *Cancer Res* 65(13): 5620–5627.
25. Egawa T, Tillman RE, Naoe Y, Taniuchi I, Littman DR (2007) The role of the Runx transcription factors in thymocyte differentiation and in homeostasis of naive T cells. *J Exp Med* 204(8):1945–1957.
26. Rudra D, et al. (2009) Runx-CBFbeta complexes control expression of the transcription factor Foxp3 in regulatory T cells. *Nat Immunol* 10(11):1170–1177.
27. Kratz E, et al. (2006) Functional characterization of the Bcl-2 gene family in the zebrafish. *Cell Death Differ* 13(10):1631–1640.
28. Plaster N, Sonntag C, Busse CE, Hammerschmidt M (2006) p53 deficiency rescues apoptosis and differentiation of multiple cell types in zebrafish flathead mutants deficient for zygotic DNA polymerase delta1. *Cell Death Differ* 13(2):223–235.
29. Hess I, Boehm T (2012) Intravital imaging of thymopoiesis reveals dynamic lymphoepithelial interactions. *Immunity* 36(2):298–309.
30. Sun L, et al. (2010) Declining expression of a single epithelial cell-autonomous gene accelerates age-related thymic involution. *Aging Cell* 9(3):347–357.
31. Cheng L, et al. (2010) Postnatal tissue-specific disruption of transcription factor FoxN1 triggers acute thymic atrophy. *J Biol Chem* 285(8):5836–5847.
32. Markert ML, et al. (2011) First use of thymus transplantation therapy for FOXN1 deficiency (nude/SCID): A report of 2 cases. *Blood* 117(2):688–696.
33. Liu F, Patient R (2008) Genome-wide analysis of the zebrafish ETS family identifies three genes required for hemangioblast differentiation or angiogenesis. *Circ Res* 103(10):1147–1154.
34. Wang L, et al. (2011) A blood flow-dependent klf2a-NO signaling cascade is required for stabilization of hematopoietic stem cell programming in zebrafish embryos. *Blood* 118(15):4102–4110.